JOURNAL OF SOLID STATE CHEMISTRY 12, 253–258 (1975)

Defects and the Electronic Properties of $Y_3Fe_5O_{12}$*

P. K. LARSEN AND R. METSELAAR

Philips Research Laboratories, Eindhoven, The Netherlands

Received July 3, 1974

The electrical and the optical absorption properties of yttrium iron garnet (YIG) are investigated. The stoichiometry is studied by means of lattice constant measurements and the defect mechanism is discussed. From high-temperature conductivity measurements at various oxygen pressures the band-gap energy is determined to be 2.85 eV. The influence of extrinsic impurities (Pb and Si) on the electrical conductivity and the optical absorption is investigated on thin films grown by liquid phase epitaxy. On the basis of these results and optical work by other investigators a model for the band structure of YIG is proposed and discussed.

I. Introduction

The ferrimagnetic oxide $Y_3Fe_5O_{12}$, yttrium iron garnet (YIG), is an important material for a number of technical applications. Depending on the type of application, it is used in the form of bulk single crystals, epitaxially grown thin films, or as polycrystalline sintered samples. These three forms necessarily are prepared in different ways and consequently, they differ in a number of physical properties, e.g., resistivity, optical absorption, lattice constant, and photomagnetic properties. These differences are mainly caused by variations in the concentration of point defects, including impurity ions.

In this paper some aspects of the defects in YIG will be considered with the main emphasis on recent work of the authors. After a discussion of the stoichiometry of YIG on the basis of lattice constant measurements (*1*) in section II, electrical resistivity data (*2*) and measurements of the optical absorption properties (*3*) will be discussed in sections III and IV, respectively. Finally, the consequences of the different measurements for the energy level diagram will be discussed.

II. The Stoichiometry of YIG

Due to the incongruent melting point single crystals of YIG have to be grown from a flux, usually a mixture of PbO and PbF_2. The resulting material is always contaminated with lead, silicon, and fluorine ions. The concentration of these impurities can be determined by ion specific chemical analysis. By means of an oxidimetric titration with Ce^{4+} the reducing power of the sample is determined. The result is normally expressed as a concentration of ferrous ions $[Fe^{2+}]$. (In this paper concentrations will be expressed in the number of ions per formula unit of YIG.) Correspondingly, a possible oxidizing power of the sample is expressed by $[Fe^{4+}]$. If $[Me^{2+}]$ denotes the sum of all divalent ions except $[Fe^{2+}]$ and $[Me^{4+}]$ the sum of all tetravalent ions plus the fluorine concentration one finds for nominally undoped YIG typical values $[Me^{2+}] \sim 0.02 \pm 0.01$ and $[Me^{4+}] \sim 0.02 \pm 0.005$ (*4*). (A concentration of 1 ion/formula unit corresponds to $4.22 \cdot 10^{21}$ cm^{-3}.) Furthermore, the ferrous concentration in nominally pure YIG is found to have values in the range $0 < [Fe^{2+}] \lesssim 0.03$, a value which is mostly higher than the difference $[Me^{4+}] - [Me^{2+}]$. This discrepancy is explained by the assumption of intrinsic defects, e.g., oxygen

---

* Invited paper.

vacancies or metal interstitials. From the analysis it follows that the concentration of these defects is of the same order of magnitude as the ferrous concentration. Polycrystalline material can be prepared with a much higher purity than single crystals by using wet-chemical preparation techniques. Typical values of unwanted impurities (Mg^{2+}, Ni^{2+}, Cu^{2+}, Si^{4+}....) are $[Me^{2+}] \sim [Me^{4+}] \sim 0.001$ (*1*). The ferrous concentration is, however, again found to have values of the order 10^{-2}. Thermogravimetric measurements have shown a reversible oxygen loss during a high-temperature treatment in low oxygen partial pressures (*5*). We therefore assume that oxygen vacancies are created during the necessary high-temperature process at the preparation of YIG.

If Fe^{2+} is formed according to the reaction

$$(\text{Donor}^{\bullet}\cdot\text{electron}) + Fe^{3+} \rightleftarrows \text{Donor}^{\bullet} + Fe^{2+}, \tag{1}$$

and assuming that $[Fe^{2+}] = [V_O^{\bullet}]$ we have

$$Fe^{3+} + O'' \rightleftarrows \tfrac{1}{2}(O_2)_g + V_O^{\bullet} + Fe^{2+} + \Delta H. \tag{2}$$

Here ΔH is the enthalpy of the reaction.

From this equation it follows

$$[V_O^{\bullet}] \propto P_{O_2}{}^{-m}, \qquad \text{with } m = \tfrac{1}{4}. \tag{3}$$

It is also possible that doubly ionized oxygen vacancies or interstitial cations act as donors, in which cases the constant m in Eq. (3) assumes different values.

At low defect concentrations a change in donor concentration is accompanied by a linear change in the lattice constant a_0, and from Eq. (3) we then expect

$$a_0 = A + B \cdot P_{O_2}{}^{-m}, \tag{4}$$

where m depends on the reaction which actually dominates and A and B are constants. Indeed the experiments on polycrystalline samples can be described with Eq. (4), where $m = 1/6$, corresponding to compensation by doubly ionized oxygen vacancies (*1*). These assumptions are further supported by an investigation of the photomagnetic effect in YIG, i.e., the light induced change in the magnetic susceptibility (*1*). The uncertainty in the experimental data is too large, however, to exclude with certainty other compensation mechanisms.

Measurements of the lattice constant can also be used to estimate the enthalpy of the underlying defect reaction. From Eq. (2) we get for the equilibrium constant K_2

$$K_2(T) = [V_O^{\bullet}]\,[Fe^{2+}]\,P_{O_2}^{\frac{1}{2}} = K_2{}^{\circ} \cdot e^{-\Delta H/kT}. \tag{5}$$

At a constant oxygen pressure and assuming $[V_O^{\bullet}] = [Fe^{2+}]$ we have

$$[V_O^{\bullet}] \propto e^{-\Delta H/2kT}. \tag{6}$$

As mentioned above, we may write $(a_T - a_{T0}) \propto [V_O^{\bullet}]$. Here a_T is the lattice constant of a sample quenched to room temperature after annealing at a temperature T under a defined partial oxygen pressure. a_{T0} is the lattice constant of a sample with a negligible concentration of defects. From Eq. (6) it follows that a plot of $\log(a_T - a_{T0})$ vs T^{-1} gives a straight line with a slope $\Delta H/2k$. Generally the slope will be $n\Delta H/k$, where n depends on the actual defect reaction, e.g., compensation by $V_O^{\bullet\bullet}$ gives $n = 1/3$.

Figure 1 gives the experimental results for YIG powders after a heat treatment in 1 atm of oxygen. The main difficulty is the determination of the reference value a_{T0}. Here too, we used a sample which was cooled very slowly from 1200°C to room temperature. For this sample we found $a_{T0} = 12.3755$ Å. The slope of the resulting line in Fig. 1 gives $n\Delta H = 1.6$ eV.

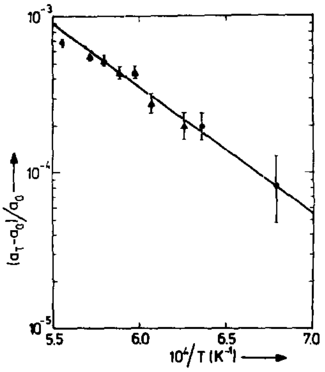

FIG. 1. Relative change in lattice parameter of YIG which was quenched to room temperature after annealing in an oxygen atmosphere at temperature T(K). Reference $a_0 = 12.3755$ Å. Circled points are measurements of the authors, triangles denote measurements of Paladino and Maguire (*6*).

These experiments show that the ferrous concentration in YIG can be explained by intrinsic defects acting as donors. Though the experiments do not allow a distinction between anion vacancies or cation interstitials we regard the formation of oxygen vacancies as the most probable mechanism.

More direct information on the defects discussed above will be presented in the following sections.

III. High Temperature Electrical Measurements

In section II we have seen that pure YIG always contains some defects of donor type and in accordance with this undoped YIG is always found to be *n*-type. By doping with acceptors like Ca one can produce *p*-type garnet. The donor concentration in such materials can be regulated by means of a high temperature annealing treatment. We have used this to study the intrinsic electrical properties of YIG (*2*). Measurements were performed on YIG samples doped with Mg or Ca. At $P_{O_2} = 1$ atm, the samples are *p*-type. At temperatures sufficiently high to enable oxygen diffusion through the sample, a lowering of P_{O_2} causes a decrease of the conductivity σ due to an increased compensation of the acceptors. At each temperature there exists a pressure $P_{O_2}{}^{\text{min}}$ where the conductivity reaches a minimum σ_{min}. At sufficiently low oxygen pressures the negative charge carriers dominate and the samples become *n*-type. This behavior can be analysed conveniently by plotting the logarithm of the conductivity vs the Seebeck coefficient α. It has been shown by Jonker (*7*) that in the presence of intrinsic effects a pear-shaped curve results. Extrinsic regions are characterised by straight lines in such a plot. From our experimental curves (*2*) it is immediately clear that we are in the region of intrinsic conduction.

More information can be derived from the position of σ_{min} as a function of temperature. We have

$$\sigma_{\text{min}} = 2e(\mu_+ \mu_- N_+ N_-)^{1/2} \exp(-E_i/2kT). \quad (7)$$

Here N and μ are the density of states and the mobility, respectively, while + and − denote holes and electrons. The band gap energy E_i can be determined from Eq. (7) if the temperature dependence of N and μ are known. Since no firm evidence exists for either hopping or band conduction we have calculated E_i under both assumptions. Generally the band gap energy itself obeys a relation $E_i(T) = E_i(0) - \beta T$, where β is a constant.

Assuming band conduction in both *n*-type and *p*-type regions we find for the Ca and Mg doped YIG samples a value $E_i(0) = 2.85$ eV. If we instead assume a hopping conduction we obtain $E_i(0) + U_+ + U_- = 3.15$ eV, where U_+ and U_- are the activation energies for the hopping motion of the positive and negative carriers. This gives 3.15 eV as an upper limit for the band gap energy.

We can compare our results from the electrical measurements with data from optical measurements. From the optical absorption and Faraday rotation at 6 K, Wettling et al. (*8*) find a transition at 2.88 eV, which they identify with the first charge transfer band. From similar measurements at 300 K Wittekoek et al. (*9*) obtain a value of 2.81 eV. These results are in good agreement with our determination of $E_i(0)$ using the band model. If the hopping model holds for YIG then the comparison of the optical and electrical data gives a value for $U_+ + U_- \approx 0.27$ eV.

IV. Electrical and Optical Absorption Properties of LPE-Films

Since the development of the liquid phase epitaxy (LPE) growth method we have a convenient way to produce single crystalline thin films of YIG. Such films can be used to study the optical absorption properties in the region of the strongly absorbing crystal field transitions($0.6\,\mu m < \lambda < 1\,\mu m$). Films of about 5 μm thickness were grown on a 200 μm thick substrate of $Gd_3Ga_5O_{12}$ by dipping in a supercooled melt. The flux mainly consisted of a $PbO:B_2O_3$ mixture. It is unavoidable that some Pb is incorporated in the garnet lattice. The amount of lead can be varied from about 0.02 to 0.5 by decreasing the growth temperatures T_g of the films from 960 to 780°C (*3*).

Since lead is present in the form of Pb^{2+}, we can easily vary the acceptor concentration.

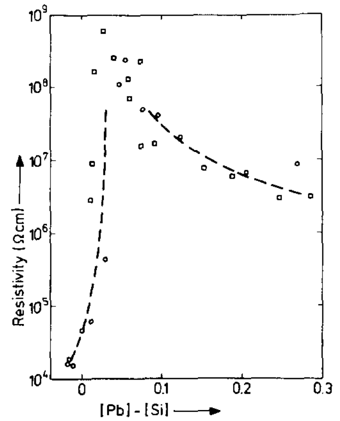

FIG. 2. The resistivity at 300 K of two series of YIG films grown by liquid phase epitaxy as a function of the analyzed difference concentration in lead and silicon. Films of series II (circles) contain 10 times more silicon than films of series I (squares).

By adding different amounts of silicon to the flux we can also adjust the donor concentration. The only factor unknown is the concentration of intrinsic defects like oxygen vacancies. It is of interest therefore to investigate the behavior of the electrical and optical properties of these films as a function of the donor–acceptor concentration. Figure 2 shows the resistivity of two series of films as a function of the concentration difference [Pb] − [Si]. The absolute values of the silicon content in series I are about 0.1 of those in series II. For both series a maximum in the resistivity is found at approximately the same concentration difference. This maximum nearly coincides with a change from *n*-type to *p*-type conductivity which for both series occurs for $[\mathrm{Pb}] - [\mathrm{Si}] \approx 0.06$. For *n*-type films the activation energy of the conductivity is about 0.3 eV, for the *p*-type films the energy slightly varies with the growth temperature from 0.33 eV to 0.40 eV. The optical absorption coefficient k shows also a marked dependence on the growth conditions. The absorption increases with decreasing growth temperatures, i.e., with increasing excess of acceptors.

The results of the optical and electrical measurements can be understood for the greater part if we assume that the tetravalent silicon is charge compensated by divalent lead. Our results are in this respect analogous to those obtained by Wood and Remeika (*10*) on YIG crystals doped with either Ca^{2+} or Si^{4+}. As for the bulk crystals we have to assume that an appreciable concentration of intrinsic defects of donor type is present. A detailed analysis of the measurements as given in Ref. (*3*) shows that the concentration of oxygen vacancies can be of the order $[V_{\mathrm{O}}^{\cdot\cdot}] \approx 0.03$, i.e., of the same order of magnitude as found for bulk single crystals and polycrystalline samples. For a sufficiently large excess of lead viz $[\mathrm{Pb}] - [\mathrm{Si}] > 0.09$ the films exhibit a broad absorption band superposed on the crystal field peaks of the garnet. The wavelength dependence is rather structureless but with indications of a peak in the wavelength range 0.7–0.8 μm (1.8–1.55 eV) and a strong peak below 0.55 μm (above 2.2 eV). The rather broad spectrum indicates that the transitions involve band states. In section V we shall discuss these transitions in more detail.

To investigate the influence of ferrous ions on the absorption constant we have measured films with an excess of Si. Our results are rather similar to those of Dillon et al. (*11*) for bulk crystals with the exception that we do not find a broad peak at about 1.3 eV but more a broad plateau with a slowly increasing absorption constant between the energies 1.2 and 1.6 eV.

V. Band Structure of YIG

When studying the band structure of YIG one encounters the same problems as in other transition metal oxides like, e.g., NiO. The problems are caused by the presence of the *d*-levels, which may form more or less localized bands. As in normal semiconductors there also are broad band-like states, namely a valence band which mainly is derived from oxygen 2*p*-orbitals and a conduction band derived from iron 4*s*-states or yttrium 5*s*-states. The energy gap between these broad bands is generally large in the transition metal oxides. From optical reflection measurements on YIG Galuza et al. (*12*) showed the presence of very strong bands with absorption coefficients as high as $9 \times 10^5\ \mathrm{cm}^{-1}$ at 10.5 and 18.2 eV. The presence of a band near 10 eV with a high oscillator strength is confirmed by an analysis of the dispersion curves of a number of garnets (*13*). The high value of the absorption coefficient agrees with dipole allowed $p \rightarrow s$ transitions.

At energies below 10 eV charge transfer transitions with smaller oscillator strengths are observed. As mentioned in section III the energetically lowest lying band is situated at 2.81–2.88 eV (*8*, *9*). In view of the high Faraday rotation and the low oscillator strength Wittekoek et al. (*9*) attributed this band to the parity forbidden transition between oxygen 2*p*-states and iron 3*d*-states mainly octahedral in character. At 3.35 eV another charge transfer transition is found and because of its very low Faraday rotation and the high oscillator strength this band is assigned to a symmetry allowed transition from $O(2p) \rightarrow Fe(3d)$ states mainly tetrahedral in character. However, the possibility of Fe–Fe charge transfer cannot be excluded (*14*). From a derivative of the absorption spectrum Wemple et al. (*15*) and Blazey (*16*) find an extra band at 3.16 eV which they also attribute to a charge transfer transition. Our high temperature conduction measurements gave a value of 2.85 eV (or a value smaller than 3.16 eV) for the energy gap. This value agrees with the energy of the lowest charge transfer band. We therefore assume that the states involved in the optical transition can be identified with the valence and conduction band states. This identification implies that the *n*-type conduction takes place in a narrow band derived from Fe(3*d*)-orbitals mainly octahedral in character. If the degree of localization is high, occupied states in this band are denoted as Fe^{2+} states.

Let us now consider our model further in connection with the experimental results. The half width of the charge transfer absorption band at 2.88 eV is about 0.3 eV, i.e., more than 10 times *kT*. This means that at least one of the two levels involved in this transition has to be broad. Fontana and Epstein (*17*) interpreted their measurements of a temperature independent Hall mobility in Si-doped YIG (*n*-type) in terms of band conduction. The activation energy of 0.3 eV should in this case be the ionization energy of the charge carriers from the Si-donors. On the other hand, Elwell and Dixon (*18*) interpreted the observed temperature independence of the Seebeck coefficient in Hf-doped YIG in terms of the hopping model. In this case the activation energy of the conductivity is ascribed to the activation energy of the drift mobility solely. From previous investigations by the present authors on polycrystalline *n*-type YIG there is evidence that the temperature dependence of the conductivity in these samples is mainly due to an ionization of the charge carriers (*19*). The activation energy was rather high, 0.56–0.9 eV, and these experiments therefore do not exclude a small activation energy of the mobility.

Also for *p*-type samples the conduction mechanism is uncertain. For Ca or Pb doped YIG one finds an activation energy of 0.35–0.40 eV near room temperature. However, from the absorption spectrum of YIG with a lead excess more information is obtained. This absorption is due to transitions from the valence band to the Pb acceptor level (*3*). The observation of a broad structureless band, starting at about 0.6 eV or less, indicates the presence of a broad valence band.

In Fig. 3 we propose an energy level diagram for YIG based on the information discussed above. The oxygen 2*p* band (valence band) is a normal one-electron band, which

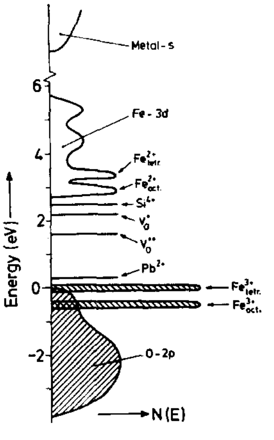

FIG. 3. Proposed density of states diagram for yttrium iron garnet. Hatched areas denote states filled at $T = 0$ K. The zero point of the energy scale is set at the top of the valence band.

is filled at $T = 0$ K. The two Fe^{3+} bands form narrow bands due to the localized nature of these states and are also filled at $\mathrm{T} = 0$ K. These two narrow bands have to be situated at a lower energy than the energy level of the Pb acceptor, because otherwise the extra absorption in YIG:Pb cannot be explained. The relative position of the top of the oxygen $2p$-band and the Fe^{3+}-bands still has to be determined. In Fig. 3 we have situated the $\mathrm{Fe}^{3+}_{\mathrm{tetr}}$ band at the top of the oxygen band (which is taken as zero on the energy scale). In accordance with our identification of the conduction band with the lowest $\mathrm{Fe}^{2+}_{\mathrm{oct}}(t_{2g})$ level, this level is situated at approximately 2.9 eV, while the $\mathrm{Fe}^{2+}_{\mathrm{tetr}}(e)$ level is placed near 3.4 eV. We have drawn two broad bands at higher energies denoting the $\mathrm{Fe}^{2+}_{\mathrm{oct}}(e_g)$ and $\mathrm{Fe}^{2+}_{\mathrm{tetr}}(t_2)$ levels. These levels probably are the final states for the strong charge transfer transitions which are observed in the absorption spectra above 3.4 eV (*15*, *16*). Above about 8 eV the broad conduction band formed by metal s-states is drawn.

In the energy gap between the valence band and the $\mathrm{Fe}^{2+}_{\mathrm{oct}}$ band some possible donor levels and the Pb acceptor level are shown. The $V_{\mathrm{O}}^{\bullet}$ and $V_{\mathrm{O}}^{\bullet\bullet}$ are assumed to be deeper donors than Si^{4+} because we always find a smaller conductivity with a higher activation energy in oxygen deficient than in Si doped YIG. The picture of the donor states given here is, however, very schematically because donor complexes $(\mathrm{donor}^{\bullet} \cdot \mathrm{Fe}^{2+}_{\mathrm{oct}})$ can also be formed.

From the discussion it will be clear that a further identification of the energy level diagram awaits supplementary experimental data.

Conclusion

From different types of measurements, i.e., lattice constant measurements, electrical measurements, and optical absorption measurements the importance of intrinsic point defects, probably oxygen vacancies, has been shown. The defect concentration typically has values of 0.01–0.03 per formula unit. The band gap energy determined by the electrical measurements at high temperatures and the optical absorption of YIG:Pb have together with optical work by other investigators been used to construct an energy level diagram for YIG. In this diagram the two Fe^{3+}-bands, which are filled at $T = 0$ K, are situated energetically near to or below the top of the oxygen $2p$ valence band.

Acknowledgments

The authors wish to thank Dr. J. Robertson for the supply of the garnet films, Dr. Th. J. A. Popma, Dr. P. F. Bongers, and Dr. S. Wittekoek for discussions and Mr. P. Verburg and Mr. M. A. H. Huyberts for technical assistance.

References

1. R. Metselaar and M. A. H. Huyberts, *J. Phys. Chem. Solids* **34**, 2257 (1973).
2. R. Metselaar and P. K. Larsen, *Solid State Comm.* **15**, 291 (1974).
3. P. K. Larsen and J. Robertson, *J. Appl. Phys.* **45**, 2867 (1974).
4. E. Haberkamp and W. Tolksdorf, unpublished.
5. R. Metselaar and M. A. H. Huyberts, unpublished.
6. A. E. Paladino and E. A. Maguire, *J. Amer. Ceram. Soc.* **53**, 98 (1970).
7. G. H. Jonker, *Philips Res. Repts.* **23**, 131 (1968).
8. W. Wettling, B. Andlauer, P. Koidl, J. Schneider, and W. Tolksdorf, *Phys. Status Solidi* **B59**, 63 (1973).
9. S. Wittekoek, Th. J. A. Popma and J. M. Robertson, *AIP Conf. Proc.* **18**, 944 (1974).
10. D. L. Wood and J. P. Remeika, *J. Appl. Phys.* **37**, 1232 (1966).
11. J. F. Dillon, Jr., E. M. Gyorgy, and J. P. Remeika, *J. Appl. Phys.* **41**, 1211 (1970).
12. A. I. Galuza, V. V. Eremenko, and A. P. Kirichenko, *Sov. Phys. Solid State* **15**, 407 (1973).
13. S. H. Wemple and W. J. Tabor, *J. Appl. Phys.* **44**, 1395 (1973).
14. R. P. van Stapele and S. Wittekoek. Private communication.
15. G. H. Wemple, S. L. Blank, J. A. Seman, and W. A. Biolsi, *Phys. Rev. B.* **9**, 2134 (1974).
16. K. W. Blazey, *AIP Conf. Proc.* **10**, 735 (1972).
17. R. E. Fontana and D. J. Epstein, *Mater. Res. Bull.* **6**, 959 (1971).
18. D. Elwell and A. Dixon, *Solid State Comm.* **6**, 585 (1968).
19. P. K. Larsen and R. Metselaar, *Phys. Rev. B* **8**, 2016 (1973).